Stannaborate Chemistry: Nucleophilic Substitution at the Cluster Sphere

Benno Ronig,[b] Torsten Bick,[b] Ingo Pantenburg,[b] and Lars Wesemann*[a]

Keywords: Boranes / Boron / Tin / Nucleophilic substitution

Nucleophilic substitution at (γ-chloropropyl)stanna-*closo*-dodecaborate $[Cl(CH_2)_3SnB_{11}H_{11}]^-$ with RLi [R = Ph, $Me_2NC_6H_4$, ferrocenyl (Fc)] and RMgBr (R = vinyl, benzyl) affords the substitution products containing the anion $[RSnB_{11}H_{11}]^-$. The reaction products have been characterized by elemental analysis, NMR spectroscopy and in the cases where R = Ph, $Me_2NC_6H_4$, Fc and vinyl by X-ray structure analysis.

Introduction

The nucleophilic substitution at tin(IV) halides with organic derivatives of electropositive elements is a very important method for the formation of new tin−carbon bonds.[1] In another possible route, triorganylstannyl metal compounds find extensive use for the preparation of Sn−C units.[1] In this context, the nucleophilic substitution at tetraorganotin compounds with basic nucleophilic reagents such as alkyl- or phenyllithium is a less frequently used method and is more well-known in the case of the transmetallation reactions and the preparation of organolithium, organoboron or organocopper compounds. Thus, a straightforward procedure is the formation of vinyllithium by reaction between tetravinyltin and four equivalents of phenyllithium.[2] The equilibrium of this kind of reaction is driven completely to the right side when the stability of the formed organolithium compound is larger than that of the starting lithium reagent.

Currently we are exploring the chemistry of a heteroborate, the stanna-*closo*-dodecaborate $[SnB_{11}H_{11}]^{2-}$ dianion, which is accessible in amounts of about five grams following a two step procedure.[3] The investigation of the ligand abilities of this cluster with respect to its cocatalytic properties and use in metal cluster formation are of interest to us.[4,5] Furthermore, we are studying organic transformation reactions at the cluster sphere. So far it is well established that the dianion $[SnB_{11}H_{11}]^{2-}$ acts as a nucleophile with alkyl iodides or reactive alkyl bromides like propargyl bromide.[6] The reaction with alkyl iodides is equivalent to an oxidation of the tin nucleus deduced from ^{119}Sn NMR and Mössbauer spectroscopy studies.[7] In this publication, we present the nucleophilic substitution at the tin center in alkylated stanna-*closo*-dodecaborate derivatives.

[a] Institut für Anorganische Chemie II, Universität Tübingen, Auf der Morgenstelle 18, 72076 Tübingen, Germany
Fax: (internat.) + 49-7071-5306
E-mail: lars.wesemann@uni-tuebingen.de
[b] Institut für Anorganische Chemie, Universität zu Köln, Greinstr. 6, 50939 Köln, Germany

Results and Discussion

(γ-Benzenesulfonyloxy)alkyltributyltin derivatives (Scheme 1) have been used successfully for the synthesis of cyclopropane derivatives.[8] In the stereoselective reaction with *n*-butyllithium, the products are cyclopropane, tetrabutyltin and lithium phenylsulfonate (Scheme 1).[9]

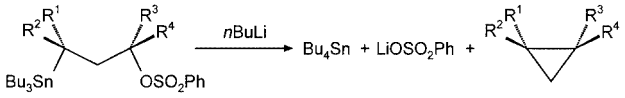

Scheme 1. Stereoselective formation of alkylated cyclopropane derivatives by nucleophilic attack at the tin atom in (γ-benzenesulfonyloxy)alkyltributyltin compounds (R^1−R^4 = alkyl substituent)

In analogy to this cyclopropane formation reaction, we have treated (γ-chloropropyl)stanna-*closo*-dodecaborate (**1**) with a variety of nucleophiles (Scheme 2 and 3). It turned out that the very reactive lithium reagents attack the tin center at room temperature and the desired products **2**, **3** and **4** can be isolated in high yield. Grignard reagents, however, have to be refluxed in THF in order to react successfully at the tin vertex.

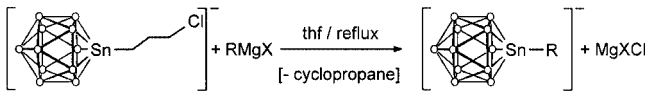

$[Bu_3MeN][Cl(CH_2)_3(SnB_{11}H_{11})]$ (1) $[Bu_3MeN][R(SnB_{11}H_{11})]$

Scheme 2. Nucleophilic substitution at the tin vertex in (γ-chloropropyl)stanna-*closo*-dodecaborate with lithium organic reagents: R = Ph **2**, $[p\text{-}Me_2NC_6H_4]$ **3**, Fc **4**

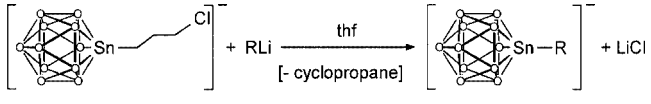

$[Bu_3MeN][Cl(CH_2)_3(SnB_{11}H_{11})]$ (1) $[Bu_3MeN][R(SnB_{11}H_{11})]$

Scheme 3. Nucleophilic substitution in refluxing THF: R = $CH_2C_6H_5$ **5**, H_2CCH **6**

Reaction of an alkyl-substituted stanna-*closo*-dodecaborate derivative $\{[RSnB_{11}H_{11}]^-\}$ with a nucleophile $[R']^-$ would lead to an equilibrium mixture between $\{[RSnB_{11}H_{11}]^- + [R']^-\}$ and $\{[R'SnB_{11}H_{11}]^- + [R]^-\}$ with the ratios dependent on the stability of the respective anions $[R']^-$ and $[R]^-$. On use of the γ-chloropropyl substituent, this reaction is driven completely to the right side, since the leaving group cyclopropane and the chloride anion are formed. In order to use the γ-chloropropyl substituent as a protecting group, we treated the alkylated cluster **1** with hydride as the nucleophile. From this reaction the unsubstituted cluster **7** was isolated in high yield (Scheme 4).

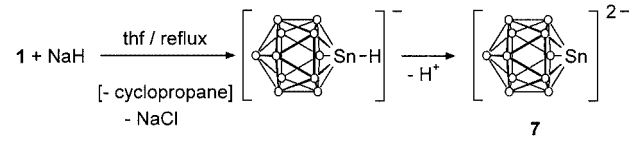

7

Scheme 4. Substitution reaction with a hydride nucleophile followed by deprotonation

However, so far we were not able to isolate the postulated, protonated cluster anion $[HSnB_{11}H_{11}]^-$ from this reaction or by treatment of **7** with a mineral acid. The air-stable substitution products **2**−**6** have been characterized by elemental analysis, NMR spectroscopy and in the cases of **2**−**4** and **6** by X-ray crystal structure analysis. In the ^1H NMR spectrum of the substitution products, the absence of the characteristic signals of the $Sn-(CH_2)_3-Cl$ group is a very good indicator for a successful reaction. The ^{11}B NMR spectrum of the starting materials and the products exhibit almost no change; two signals around δ = −11 and −16 ppm (B12, B2−B11) are characteristic for the substituted cluster. In order to confirm the geometry of the product salts, X-ray crystal structure determinations have been

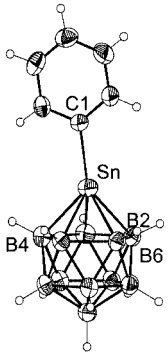

Figure 1. Molecular structure of the anion of $[Bu_3MeN][PhSnB_{11}H_{11}]$ (**2**) in the solid state; interatomic distances in [pm] (with estimated standard deviations in parentheses): Sn−C 210.7(3), Sn−B2 228.1(3), Sn−B3 228.4(3), Sn−B4 228.6(3), Sn−B5 228.7(3), Sn−B6 229.1(3); thermal ellipsoids are shown at the 50 % probability level

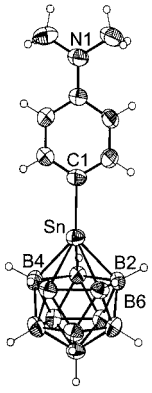

Figure 2. Molecular structure of the anion of $[Bu_3MeN][Me_2NC_6H_4SnB_{11}H_{11}]$ (**3**) in the solid state; interatomic distances in [pm] (with estimated standard deviations in parentheses): Sn−C 210.0(4), Sn−B2 228.7(5), Sn−B3 228.8(5), Sn−B4 229.0(5), Sn−B5 229.4(5), Sn−B6 229.7(5); thermal ellipsoids are shown at the 50 % probability level

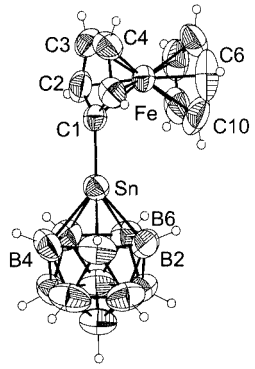

Figure 3. Molecular structure of the anion of $[Bu_3MeN][FcSnB_{11}H_{11}]$ (**4**) in the solid state; thermal ellipsoids are shown at the 50 % probability level; interatomic distances in [pm] (with estimated standard deviations in parentheses): Sn−C 206.8(3), Sn−B2 225.5(5), Sn−B3 227.4(5), Sn−B4 227.6(5), Sn−B5 228.1(5), Sn−B6 228.4(4), Fe−C1 202.9(4), Fe−C2 202.9(4), Fe−C3 203.6(4), Fe−C4 203.6(4), Fe−C5 204.0(4), Fe−C6 200.9(4), Fe−C7 201.3(4), Fe−C8 201.4(5), Fe−C9 201.8(4), Fe−C10 201.8(5)

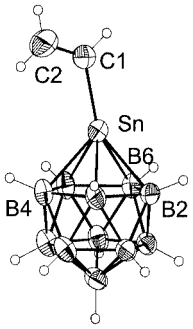

Figure 4. Molecular structure of the anion of $[Bu_3MeN][(H_2CCH)SnB_{11}H_{11}]$ (**6**) in the solid state; thermal ellipsoids are shown at the 50 % probability level; interatomic distances in [pm] (with estimated standard deviations in parentheses): Sn−C1 207.7(5), C1−C2 129.6(8), Sn−B2 229.1(5), Sn−B3 229.3(5), Sn−B4 229.5(6), Sn−B5 230.4(5), Sn−B6 230.3(5)

carried out. In Table 1, details of the X-ray structure solutions are listed and in Figures 1−4, the structures of the respective anions in the solid state are depicted.

The results of the crystal structure determinations are consistent with the findings of elemental analysis and NMR spectroscopy. The geometries of the substituted clusters exhibit no peculiarities and the Sn−B and B−B interatomic distances are in the range known from other derivatives. The deviation from linearity of the angle C−Sn−(antipodal)B (**2** 171.7°, **3** 175.8°, **4** 178.1°, **6** 167.2°) is a common effect in these substituted stannaborate derivatives and can be explained by packing forces in the solid state.

Conclusion

With this straightforward substitution at the tin center in γ-chloropropyl-substituted stanna-*closo*-dodecaborate, a method for the linkage of an aromatic cluster anion with π-systems like the phenyl, ferrocenyl or vinyl moiety has been found.

Experimental Section

General: All manipulations were carried out under dry N_2 in Schlenk glassware; solvents were dried and purified by standard methods and stored under N_2. NMR spectroscopy was performed on a Bruker AC 200 (^{1}H: 200 MHz, int. TMS; ^{11}B{^{1}H}: 64 MHz, ext. $BF_3{\cdot}Et_2O$). Elemental analysis was carried out by the Institut für Anorganische Chemie der Universität zu Köln, on a Heraeus C,H,N,O rapid elemental analyser.

$[Bu_3MeN][PhSnB_{11}H_{11}]$ (2): $[Bu_3MeN][H_{11}B_{11}SnC_3H_6Cl]$ (368 mg, M_r = 526.64 g/mol, 0.699 mmol) was dissolved in 20 mL THF and treated with an excess of phenyllithium (in Et_2O) at −78 °C. After stirring the solution overnight at room temperature, volatiles were removed in vacuo and the residue was washed with H_2O (20 mL). The product was dissolved in CH_2Cl_2, filtered and crystallized by slow diffusion of *n*-hexane to give **2** (234 mg, M_r = 526.21 g/mol, 0.445 mmol, 64 %). ^{1}H NMR (CD_2Cl_2): δ = 0.98 (t, 9 H, ^3J = 7.3 Hz, CH_2CH_3), 1.41 (m, 6 H, CH_2CH_3), 1.64 (m, 6 H, $CH_2CH_2CH_3$), 3.00 (s, 3 H, NCH_3), 3.16 (m, 6 H, NCH_2), 7.55 (m, 5 H, C_6H_5) ppm. ^{11}B{^{1}H} NMR (CD_2Cl): δ = −11.1 (s, B12), −16.4 (s, B2−B6 and B7−B11). $C_{19}H_{46}B_{11}NSn$ (526.21): calcd. C 43.37, H 8.81, N 2.66; found C 43.51, H 8.82, N 2.79.

$[Bu_3MeN][Me_2NC_6H_4SnB_{11}H_{11}]$ (3): $[Bu_3MeN][H_{11}B_{11}SnC_3H_6Cl]$ (477 mg, M_r = 526.64 g/mol, 0.906 mmol) was dissolved in 20 mL THF and treated with an excess of [*p*-$Me_2NC_6H_4Li$] in Et_2O at −78 °C. After stirring the solution overnight at room temperature, volatiles were removed in vacuo and the residue was washed with H_2O (20 mL). The product was dissolved in CH_2Cl_2, filtered and crystallized by slow diffusion of *n*-hexane to give **3** (186 mg, M_r = 569.28 g/mol, 0.327 mmol, 36 %). ^{1}H NMR (CD_2Cl_2): δ = 1.00 (t, 9 H, ^3J = 7.3 Hz, CH_2CH_3), 1.41 (m, 6 H, CH_2CH_3), 1.66 (m, 6 H, $CH_2CH_2CH_3$), 2.92 [s, 6 H, $C_6H_4N(CH_3)_2$], 3.01 (s, 3 H, NCH_3), 3.19 (m, 6 H, NCH_2), 7.20 (m, 4 H, C_6H_4) ppm. ^{11}B{^{1}H} NMR (CD_2Cl_2): δ = −12.1 (s, B12), −16.9 (s, B2−B6 and B7−B11). $C_{21}H_{51}B_{11}N_2Sn$ (569.28): calcd. C 44.31, H 9.03, N 4.92; found C 42.99, H 8.95, N 4.71.

$[Bu_3MeN][FcSnB_{11}H_{11}]$ (4): $[Bu_3MeN][H_{11}B_{11}SnC_3H_6Cl]$ (500 mg, M_r = 526.64 g/mol, 0.949 mmol) was dissolved in THF at −78 °C and treated with a solution of $Li[C_5H_4FeC_5H_5]$ (546 mg, M_r = 562.67 g/mol, 0.889 mmol) in THF (20 mL). After stirring the solution overnight at room temperature, volatiles were removed in vacuo and the residue was washed with H_2O (20 mL). The product was dissolved in CH_2Cl_2, filtered and crystallized by slow diffusion of *n*-hexane to give **4** (423 mg, M_r = 634.13 g/mol, 0.667 mmol, 75 %). ^{1}H NMR (CD_2Cl_2): δ = 1.02 (t, 9 H, ^3J = 7.8 Hz, CH_2CH_3), 1.48 (m, 6 H, CH_2CH_3), 1.66 (m, 6 H, $CH_2CH_2CH_3$), 3.01 (s, 3 H, NCH_3), 3.20 (m, 6 H, NCH_2), 4.37 (s, 5 H, FeC_5H_5), 4.52 [s, 2 H, SnC-$(CH)_2$-$(CH)_2$], 4.60 [s, 2 H, SnC-$(CH)_2$-$(CH)_2$] ppm. ^{13}C{^{1}H} NMR (CD_2Cl): δ = 13.8 (CH_2CH_3), 20.1 (CH_2CH_3), 24.7 ($CH_2CH_2CH_3$), 49.5 (NCH_3), 62.5 (NCH_2), 70.4 (FeC_5H_5), 72.1 [SnC-$(CH)_2$-$(CH)_2$], 75.1 [SnC-$(CH)_2$-$(CH)_2$] ppm. ^{11}B{^{1}H} NMR (CD_2Cl_2): δ = −12.6 (s, B12), −17.3 (s, B2−B6 and B7−B11). $C_{23}H_{50}B_{11}FeNSn$ (634.13): calcd. C 43.56, H 7.95, N 2.21; found C 43.35, H 8.05, N 2.25.

$[Bu_3MeN][PhCH_2SnB_{11}H_{11}]$ (5): $[Bu_3MeN][H_{11}B_{11}SnC_3H_6Cl]$ (670 mg, M_r = 526.64 g/mol, 1.27 mmol) was dissolved in THF (30 mL) and treated with $PhCH_2MgBr$ (0.95 mL, 2 M solution in THF, 1.90 mmol). After stirring overnight at reflux temperatures, the solution turned yellow and volatiles were removed in vacuo. The residue was washed with H_2O (20 mL). The remaining residue was dissolved in EtOH, filtered and crystallized to give **5** (0.61 g, M_r = 540.24 g/mol, 1.13 mmol, 89 %). ^{1}H NMR (CD_2Cl_2): δ = 1.01 (t, 9 H, ^3J = 7.3 Hz, CH_2CH_3), 1.41 (m, 6 H, CH_2CH_3), 1.62 (m, 6 H, $CH_2CH_2CH_3$), 3.01 (s, 3 H, NCH_3), 3.17 (m, 6 H, NCH_2), 3.98 (s, 2 H, -$SnCH_2Ph$), 7.32 (m, 4 H, C_6H_4) ppm. ^{11}B{^{1}H} NMR (CD_2Cl_2): δ = −12.5 (s, B12), −17.1 (s, B2−B6 and B7−B11). $C_{20}H_{48}B_{11}NSn$ (540.24): calcd. C 44.47, H 8.96, N 2.59; found C 43.93, H 9.16, N 2.67.

$[Bu_3MeN][(H_2CCH)SnB_{11}H_{11}]$ (6): $[Bu_3MeN][H_{11}B_{11}SnC_3H_6Cl]$ (850 mg, M_r = 526.64 g/mol, 1.61 mmol) was dissolved in THF (30 mL) and treated with vinylmagnesium bromide (1.93 mL, 1 M solution in THF). After stirring the reaction mixture under reflux overnight, all volatiles were removed in vacuo. The residue was washed with H_2O (20 mL). Crystallization from CH_2Cl_2 by diffusion of *n*-hexane affords **6** (0.71 g, M_r = 476.11 g/mol, 1.49 mmol, 87 %). ^{1}H NMR (CD_2Cl_2): δ = 1.01 (t, 9 H, ^3J = 7.1 Hz, CH_2CH_3), 1.46 (m, 6 H, CH_2CH_3), 1.68 (m, 6 H,

Table 1. Crystal data and structure refinement parameters for $[Bu_3MeN][PhSnB_{11}H_{11}]$ (**2**), $[Bu_3MeN][Me_2NC_6H_4SnB_{11}H_{11}]$ (**3**), $[Bu_3MeN][FcSnB_{11}H_{11}]$ (**4**) and $[Bu_3MeN][(H_2CCH)\text{-}SnB_{11}H_{11}]$ (**6**)

	2	**3**	**4**	**6**
Empirical formula	$C_{19}H_{46}B_{11}NSn$	$C_{21}H_{51}B_{11}N_2Sn$	$C_{23}H_{50}B_{11}FeNSn$	$C_{15}H_{44}B_{11}NSn$
M_r [g/mol]	526.17	569.24	634.09	476.11
		Data Collection		
Diffractometer	STOE IPDS II	STOE IPDS II	STOE IPDS II	STOE IPDS II
Radiation	Mo-K_α (graphite monochromator, λ = 71.073 pm)			
T [K]	170(2)	170(2)	293(2)	170(2)
Index range	$-21 \le h \le 21$ $-22 \le k \le 20$ $-24 \le l \le 24$	$-14 \le h \le 14$ $-25 \le k \le 25$ $-22 \le l \le 22$	$-13 \le h \le 13$ $-15 \le k \le 15$ $-18 \le l \le 18$	$-18 \le h \le 20$ $-22 \le k \le 22$ $-21 \le l \le 24$
Rotation angle range	0° ≤ ω ≤ 180°; ψ = 0° 0° ≤ ω ≤ 180°; ψ = 90° 0° ≤ ω ≤ 180°; ψ = 135°	0° ≤ ω ≤ 180°; ψ = 0° 0° ≤ ω ≤ 122°; ψ = 90°	0° ≤ ω ≤ 180°; ψ = 0° 0° ≤ ω ≤ 114°; ψ = 90°	0° ≤ ω ≤ 180°; ψ = 0° 0° ≤ ω ≤ 58°; ψ = 90°
Increment	Δω = 2°	Δω = 2°	Δω = 2°	Δω = 2°
No. of images	270	151	147	119
Exposure time [min]	1	6	3	10
Detector distance [mm]	120	100	120	120
2θ Range [deg]	1.9−54.8	2.3−59.5	1.9−54.8	1.9−54.8
Total data collected	125815	36462	21249	47182
Unique data	6274	6080	7283	5243
Observed data	3595	3687	3931	2736
R_{merg}	0.0692	0.1324	0.0419	0.1132
Absorption correction	numerical, after crystal shape optimization[10,11]			
Transmission max/min	0.8191/0.5040	0.9435/0.5404	0.9119/0.6526	0.8904/0.7607
		Crystallographic data[12]		
Crystal size [mm]	0.3 × 0.3 × 0.2	0.2 × 0.2 × 0.1	0.5 × 0.3 × 0.05	0.5 × 0.15 × 0.15
Colour, habit	colourless, polyhedron	colourless, polyhedron	orange, plate	colourless, needle
Crystal system	orthorhombic	monoclinic	triclinic	orthorhombic
Space group	*Pbca* (no. 61)	$P2_1/n$ (no. 14)	$P\bar{1}$ (no. 2)	*Pcab* (no. 61)
a [pm]	1689.7(1)	1025.9(1)	1066.0(2)	1602.9(1)
b [pm]	1760.2(1)	1867.4(2)	1192.3(2)	1756.3(2)
c [pm]	1874.8(1)	1628.4(2)	1442.8(2)	1901.1(2)
α [°]	90	90	72.95(1)	90
β [°]	90	97.90(1)	79.51(1)	90
γ [°]	90	90	69.92(1)	90
V [nm^3]	5.5763(6)	3.0902(6)	1.6398(1)	5.3517(9)
Z	8	4	2	8
$\rho_{calcd.}$ [g·cm^{-3}]	1.253	1.224	1.284	1.182
μ [mm^{-1}]	0.925	0.841	1.218	0.957
F(000)	2176	1184	652	1968
		Structure analysis and refinement		
Structure determination	SHELXS-97[13] and SHELXL-93[14]			
No. of variables	474	317	338	258
R indexes [$I > 2\sigma(I)$][a]	R_1 = 0.0330 wR_2 = 0.0740	R_1 = 0.0480 wR_2 = 0.0941	R_1 = 0.0353 wR_2 = 0.0801	R_1 = 0.0420 wR_2 = 0.0822
R indexes [all data]	R_1 = 0.0634 wR_2 = 0.0800	R_1 = 0.0874 wR_2 = 0.1055	R_1 = 0.0774 wR_2 = 0.0900	R_1 = 0.1011 wR_2 = 0.0956
GooF [S_{obs}]	1.001	0.880	0.998	1.026
GooF [S_{all}]	0.796	1.023	0.808	0.842
Largest difference map hole/peak [e$^-$ 10^{-6} pm^{-3}]	−0.656/0.730	−0.731/0.784	−0.541/0.688	−0.500/0.531

[a] $R_1 = \Sigma| |F_o| - |F_c| | / \Sigma |F_o|$. [b] $wR_2 = [\Sigma w(F_o^2 - F_c^2)^2 / \Sigma w(F_o^2)^2]^{1/2}$, $S_2 = [\Sigma w(F_o^2 - F_c^2)^2/(n\text{-}p)]^{1/2}$, with $w = 1/[\sigma^2(F_o)^2 + (0.0529 \cdot P)^2]$ for **2**, $w = 1/[\sigma^2(F_o)^2 + (0.0573 \cdot P)^2]$ for **3**, $w = 1/[\sigma^2(F_o)^2 + (0.0512 \cdot P)^2]$ for **4** and $w = 1/[\sigma^2 (F_o)^2 + (0.0452 \cdot P)^2]$ for **6**, were $P = (F_o^2 + 2F_c^2)/3$. $F_c^* = k F_c [1 + 0.001 \cdot |F_c|^2 \lambda^3/\sin(2\theta)]^{-1/4}$.

$CH_2CH_2CH_3$), 3.02 (s, 3 H, NCH_3), 3.18 (m, 6 H, NCH_2), 6.28 (d, 1H *trans,* $^3J_{trans}$ = 19.4 Hz, CH=C*H*H), 6.52 (d, 1H *cis,* $^3J_{cis}$ = 11.7 Hz, CH=CH*H*), 6.80 (m, 1 H, C*H*=CHH) ppm. $^{11}B\{^1H\}$ NMR (CD_2Cl_2): δ = −12.4 (s, B12), −17.2 (s, B2−B6 and B7−B11). $C_{15}H_{44}B_{11}NSn$ (476.11): calcd. C 37.84, H 9.31, N 2.94; found C 37.41, H 9.61, N 2.21.

Acknowledgments

We thank the Deutsche Forschungsgemeinschaft (Schwerpunktprogramm Polyeder) and the Fonds der Chemischen Industrie for financial support.

[1] J. L. Wardell in *Chemistry of Tin* (Ed.: P. J. Smith), Blackie Academic & Professional, **1998**, pp. 95−137.
[2] D. Seyferth, M. A. Weiner, *Chemistry & Industry* **1959**, 402.
[3] R. W. Chapman, J. G. Kester, K. Folting, W. E. Streib, L. J. Todd, *Inorg. Chem.* **1992**, *31*, 979−983.
[4] L. Wesemann, S. Hagen, T. Marx, I. Pantenburg, M. Nobis, B. Drießen-Hölscher, *Eur. J. Inorg. Chem.* **2002**, 2261−2265.
[5] S. Hagen, I. Pantenburg, F. Weigend, C. Wickleder, L. Wesemann, *Angew. Chem.* **2003**, *115*, 1539−1543; *Angew. Chem. Int. Ed.* **2003**, *42*, 1501−1505.
[6] T. Marx, B. Ronig, H. Schulze, I. Pantenburg, L. Wesemann, *J. Organomet. Chem.* **2002**, *664*, 116−122.
[7] T. Marx, B. Mosel, I. Pantenburg, S. Hagen, H. Schulze, L. Wesemann, *Chem. Eur. J.* **2003**, *9*, 4472−4478.
[8] A. Krief, M. Hobe, *Tetrahedron Lett.* **1992**, *43*, 6527−6528.
[9] A. Krief, M. Hobe, *Tetrahedron Lett.* **1992**, *43*, 6529−6532.
[10] X-RED 1.22, *Stoe Data Reduction Program (C)*, **2001**, Stoe & Cie GmbH, Darmstadt.
[11] X-Shape 1.06, Crystal Optimisation for Numerical Absorption Correction (C), **1999**, STOE & Cie GmbH, Darmstadt.
[12] CCDC-218253 (for **2**), -218254 (for **3**), -218255 (for **4**) and -218256 (for **6**) contain the supplementary crystallographic data for this paper. These data can be obtained free of charge at www.ccdc.cam.ac.uk/conts/retrieving.html [or from the Cambridge Crystallographic Data Centre, 12, Union Road, Cambridge CB2 1EZ, UK; Fax: (internat.) +44-1223/336-033; E-mail: deposit@ccdc.cam.ac.uk].
[13] G. M. Sheldrick, SHELXS-97-*Program for Structure Analysis*, Göttingen, **1998**.
[14] G. M. Sheldrick, SHELXL-93-*Program for Crystal Structure Refinement*, Göttingen, **1993**.

Received October 8, 2003

